Tellus (1980) *32*, 365–375

Cone models of mountain peaks associated with atmospheric vortex streets

By JOHN W. TRISCHKA, *Syracuse University, Department of Physics, 201 Physics Building, Syracuse, New York 13210, U.S.A.*

(Manuscript received July 4; in final form November 20, 1979)

ABSTRACT

The shedding of atmospheric vortex streets from mountain peaks has been simulated in the wakes of several shapes of circular cones and one combination of two such cones placed in the uniform, unstratified flow of a wind tunnel. Conditions for vortex shedding are more favorable the steeper the slopes of the peaks. From the laboratory measurements and with the assumption of Reynolds number independence, predictions are made of the periodicities of vortex shedding from six volcanic peaks whose periodicities of vortex shedding have been determined by others from satellite photographs of wake clouds. The predicted periods agree with the measured periods in three cases and are significantly smaller in three cases. For the latter cases it is concluded that stratification has so altered the atmospheric flow that either the Strouhal number has been lowered or the barrier effect of the topographic obstacle has been considerably enhanced. It is also concluded that stratification sufficient to reduce turbulence is necessary for the existence of an extended atmospheric vortex street.

1. Introduction

A number of investigators (Chopra, 1972; Chopra and Hubert, 1964, 1965; Thomson, Gower and Bowker, 1977; Tsuchiya, 1969; Zimmerman, 1969) have analyzed the von Kármán-type vortex streets created in the stably stratified atmospheric flows downwind from island or from volcanic peaks. The vortex streets, seen as cloud patterns in satellite photographs, have the appearance of the vortex streets formed in the laboratory by circular cylinders in unstratified laminar flows at low Reynolds numbers. Some success in understanding the origins of these vortex patterns has been achieved through the use of parameters determined from the laboratory experiments with cylinders. However, the flow around cylinders cannot truly represent the three-dimensional flow over and around island and volcano obstacles. Hence, better models are needed. To date, improvements in modeling have yielded only qualitative results. Thus, Friday and Wilkins (1967), studying cylinders in stratified fluids, found no evidence that stratification favored vortex shedding. Greenly (1969) demonstrated that vortex shedding in an unstratified fluid occurred in the wake of a three-dimensional obstacle shaped like a steep-sided island.

The present paper provides quantitatively improved three-dimensional models for vortex shedding from mountain peaks whose symmetry, like that of volcanoes, approximates that of circular cones. Vortex shedding from circular cones of various shapes and characteristic slope angles was studied in the unstratified flow of a wind tunnel. To simulate the shedding from a pair of closely spaced mountain peaks, a pair of overlapping cones was used. Measurements were made of the dimensionless parameter most readily related to atmospheric measurement, the Strouhal number,

$$S = fd/u_0 \tag{1}$$

where f is the frequency of shedding, d is the characteristic dimension of the obstacle and u_0 is the wind speed. The f and u_0 values for a number of atmospheric examples are available. It is the principal intention here to see if these values are consistent with the d values appropriate to the shape of the obstacle being modeled when the assumption is made that the laboratory S values are valid for the atmospheric flow.

 0040-2826/80/040365-11$02.50/0

2. Modeling criteria

Snyder (1972) shows that the model and atmospheric prototype must be matched in Péclet number, Rossby number, Reynolds number and Richardson number. Only the Reynolds and Richardson numbers are in need of consideration here.

Reynolds number similarity cannot be established because the Reynolds numbers for the observed flows are of the order of 10^{10}, much larger than the values achieved in laboratory flows. Two approaches are used in justifying Reynolds number similarity between laboratory and prototype flows. In one, eddy viscosity ν_e is used to define an effective Reynolds number

$$R_e = u_0 d / \nu_e \tag{2}$$

The effective number, which is much lower than the actual Reynolds number, is then identified with the actual Reynolds number in a laboratory experiment. In the other approach to establishing similarity, the hypothesis of "Reynolds number independence" is used; that is, it is assumed that when the Reynolds number, defined in terms of kinematic viscosity ν, increases from that used in the laboratory to that of the atmospheric flow, there is no effect on the phenomena under investigation.

Equation (2) has been used by all those who have analyzed vortex shedding from islands and volcanoes. The assumption of Reynolds number independence is used in the present paper. General arguments favoring this choice are given by Snyder (1972). There is no empirical evidence justifying the hypothesis of Reynolds number of independence for vortex shedding from cones. However, encouragement for the hypothesis comes from experiments with cylinders, for which the combined results of several investigators (Roshko, 1954; Batham, 1973; Szeechenyi, 1975) show no substantial change in Strouhal number of $10^3 < R < 10^7$. This range of Reynolds numbers includes the crucial, supercritical range, $10^5 < R < 10^6$.

There is no possibility of Richardson number matching the present experiments. However, the importance of this number in the atmospheric examples chosen here cannot be ignored. Although the Richardson number is not available from the reports of the atmospheric investigators, temperature soundings allow the convective stability to be inferred. In all cases convectively stable air, usually in the form of an inversion, exists from the half-height level of the peak, or lower, to well above the peak at the time of observation (Lyons and Fujita, 1968; Thomson, Gower and Bowker, 1977; Tsuchiya, 1969). Lyons and Fujita (1968) describe their flow as a "stable air stream". Soundings taken before the time of observation (Tsuchiya, 1969; Thomson, Gower and Bowker, 1977) show that convectively stable air existed above and well below the tops of the peaks many hours before the vortices were observed.

The kind and degree of stratification of the atmosphere is likely to be very important for two reasons. First, stratification may influence the survival of vortices as they drift downstream from the obstacle, because stably stratified flow is expected to be less turbulent than unstable flow (Tenekes and Lumley, 1972, p. 98). Second, stable stratification is likely to influence the flow field itself, as shown in the theoretical work of Sykes (1978) whose study of stably stratified flow over a hill indicates an enhanced barrier effectiveness both vertically and horizontally. The importance of stratification in the light of the present experiments will be discussed in Section 8.

Because the atmospheric flow impinging on the volcanoes is probably turbulent to some degree, it is important to know if this turbulence must be simulated in the laboratory. Majumbar and Douglas (1970) studied the effect of turbulent flows on the Strouhal number for a circular cylinder in a wind tunnel in the range of $4000 < R < 10{,}000$. Turbulence levels were from 0.5% to 12.5%. There was no effect on the Strouhal number. The turbulence in the wind tunnel used in the present experiments was about 1%.

3. Experimental arrangements

The wind tunnel and the measuring apparatus used in these experiments have been described in detail elsewhere (Moussa, Trischka and Eskinazi, 1977). The wind tunnel has a cross section of 1.22 m high by 0.61 m wide. Smooth aluminum cones of various shapes were mounted on a horizontal flat plate with their symmetry axes perpendicular to the plate. The plate was mounted on a vertical pipe, 2.54 cm in diameter, at the center of the tunnel. The mounting plate was 43.2 cm long by 35.6 cm wide.

The center of the pipe and the axes of the cone were 17.8 cm from the leading edge of the plate. To test possible effects of boundary layer build-up on the upstream section of the plate, a cone was mounted at various distances from the leading edge of the plate. No effect on the Strouhal number was found at the Reynolds numbers reported here. Vortex shedding from the pipe was isolated by the presence of the plate and was apparent only beyond its trailing edge. A hot wire anemometer was used with a linearizer and a narrow-band real-time spectrum analyzer to make a spectral analysis of the wind speed. Spectra were plotted with an x–y recorder. Fig. 1 is such a recording. The numbers 5 and 25 are, respectively, the run number and the frequency in hertz at the point indicated.

Simple cones with straight, smooth sides had base angles of 20°, 30°, 45° and 60°. Their base angles, base diameters and heights are shown in Table 1. Most of the base angles are much larger than the slope angles of mountain peaks. Because no vortex shedding was found from cones with base angles less than 20°, the larger angles were chosen to help in assessing the influence of base angle on the shedding process. A second type of cone, more realistic in shape than the simple cone, was designed to show the effects on the Strouhal number of the lower slope angles at the lower elevations of the mountain peaks. This was a double cone, consisting of a truncated cone with one base angle capped at the truncation surface by a simple cone with a larger base angle. The second column in Table 1 gives the base angles of the two cones, starting with the lower one. The fourth column gives the height, from its base, of the truncated cone and of the upper simple cones. A third type of cone, having an exponential profile, was studied because this profile fitted most peaks better than the simple cone. The angle in column two of Table 1 is the angle made with the horizontal by a tangent to the surface at the apex of

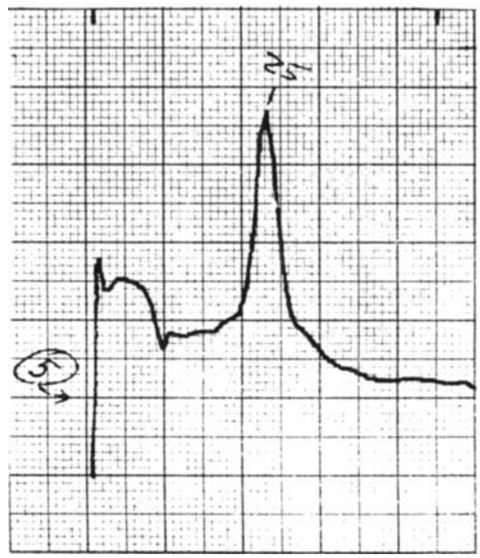

Fig. 1. Power spectrum for a 45° simple cone. 5 is the run number, and 25 is the frequency in hertz at the point indicated.

Table 1. *Cone dimensions*

Type	Angle (deg.)	Base diameter (cm)	Height (cm)	$2b$ (cm)	h_0 (cm)
Simple	20	7.62	1.40	—	—
		15.24	2.77	—	—
	30	5.08	1.47	—	—
	45	2.54	1.27	—	—
		5.08	2.54	—	—
		7.62	3.81	—	—
		15.24	7.62	—	—
	60	5.08	4.39	—	—
Double	10–20	15.24–5.08	0.89–0.91	—	—
	20–30	15.24–5.89	1.70–1.70	—	—
Exponential	30	15.24	2.54	9.68	2.79
	45	15.24	2.54	5.38	2.69
Twin	45	7.62	2.54	—	—

the cone. The equation for the profile of an exponential cone is

$$h = h_0 \exp(-r/b) \tag{3}$$

where r is the cone radius, and h is the height of the cone surface at radius r. The parameters $2b$ and h_0, as well as the base diameter and heights, are given in Table 1. The angle used to specify the cone is

$$\theta_0 = \tan^{-1}(h_0/b) \tag{4}$$

It will be noted that h_0 is greater than the height given in Table 1. This is because the cone was truncated to establish a fit, at a reasonable base diameter, with the mounting plate. Furthermore, a fit to the base plate for the 30° exponential cone led to a design in which the lower part was a 15° truncated, simple cone capped by a 30° exponential cone.

The last type of obstacle, called a twin-cone, was a pair of 45° simple cones with their 5.08 cm bases intersecting in such a way that the apex-to-apex distance was 2.54 cm and their total base length, perpendicular to the environmental flow, was 7.62 cm.

4. Scaling parameters for cones

Dimensional analysis was used to determine the dependence of the Strouhal number on the geometrical parameters of the cones and on the Reynolds number

$$R = u_0 d/\nu \tag{5}$$

In general, for a cylinder whose axis is perpendicular to a stream, S is a function only of R. For a simple cone

$$S = f(R, h/d) \tag{6}$$

where h is the cone height and d is, by choice, the base diameter. For an exponential cone

$$S = g(R, h_0/b) \tag{7}$$

For the double-cone the relation chosen was

$$S = f_d(R_1, h_1/d_1, h_2/d_1, d_2/d_1) \tag{8}$$

where $R_1 = u_0 d_1/\nu$, d_1 is the base diameter of the lower cone, d_2 is the base diameter of the upper cone, h_1 is the truncated height of the lower cone and h_2 is the height of the upper cone. The two cones used in the present experiments had $h_1 = h_2$.

No analysis was made for the twin-cone. The characteristic length used for calculating R was the base length perpendicular to the axes of the two cones.

5. Results

In all the experiments, the same shedding frequency was found at all heights from the surface of the mounting plate to the tip of the cone, and for all downstream positions of the hot-wire probe. Hence, a single Strouhal number characterized the shedding process. Besides the presence of a pronounced spectral peak, as shown in Fig. 1, evidence for the formation of a vortex street came from the observation of a double frequency downstream in the plane of symmetry of the cone.

Fig. 2 shows the relationship between Strouhal number and Reynolds number for the four simple cones. Practical reasons limited the range of Reynolds number for the 20° cone. At low Reynolds number shedding was not detectable for this cone, and it was not desirable to operate the wind tunnel at its highest speed, at the time this data was taken. The 45° cone was studied most extensively to establish the trend of the Strouhal number with Reynolds number and the effect of varying cone diameter. In the lower Reynolds number region there is a scatter of values of Strouhal number from 0.24 to 0.27 for this cone. In general, the Strouhal number decreases with increasing cone angle and, except for the 30° cone, increases with Reynolds number.

The relationships between Strouhal number and Reynolds number for the composite cones are shown in Fig. 3. Here, as for the simple cones, it is

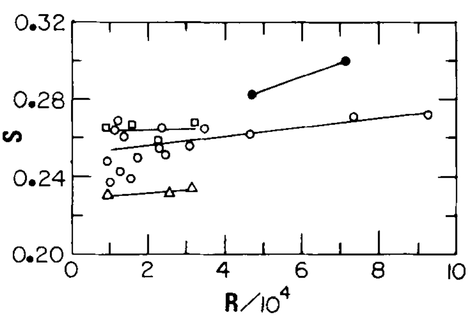

Fig. 2. Strouhal number vs Reynolds number for simple cones with various base angles. ● 20°, □ 30°, ○ 45°, △ 60°.

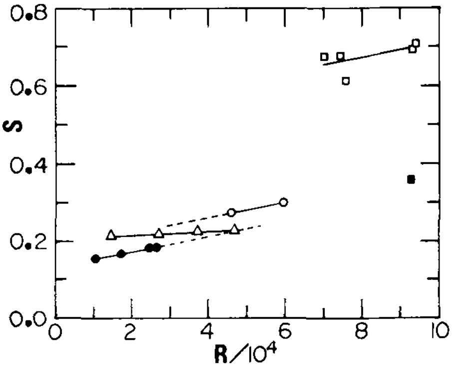

Fig. 3. Strouhal number vs Reynolds number for complex cones. ○, 30° exponential, ● 45° exponential, □ 10°–20° double, ■ 20°–30° double, △ 45° twin.

again seen that there is a trend of increasing Strouhal number with increasing Reynolds number. In the case of the exponential cones, the 30° cone has higher Strouhal numbers than the 45° cone. For the double cones, the one with smaller angles has larger Strouhal numbers. Comparison of the Strouhal number of the different types of cones is inappropriate because there is no common basis for the choice of characteristic dimensions.

For comparison with the atmospheric vortices it is useful to have a measure of the constancy of the periodicity of shedding and to assess the strength of vortices relative to some standard. The importance of the former resides in the small number, at most five of six, of atmospheric vortices observed at any one time. The hot-wire power spectrum of a cone wake, shown in Fig. 1 for one of the runs with the 20°–30° double cone, has a narrow resonance-type peak superposed on a turbulent background. A convenient measure of the constancy of shedding periodicity is the ratio $\Delta f/f$, the ratio of the width of the resonant peak at half maximum, Δf, to the central frequency f. This ratio was independent of probe position in all three directions in the wake for several diameters downstream. A rough relative measure of the strength of vortex shedding is the ratio of the area under the peak above the turbulent background to the area of the turbulent background over the same frequency region. To approximate this, $\Delta f/f$ was multiplied by the ratio Pk/Turb, the ratio of the height of the peak above the turbulent background to the turbulent background. The peak height chosen was the largest one found when the wake was explored in all three

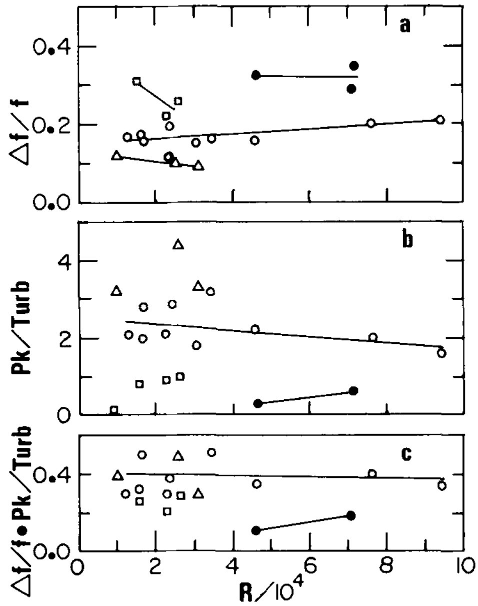

Fig. 4. Variation with Reynolds number of quantities related to vortex periodicity fluctuations. $\Delta f/f$, and vortex shedding strength, $(\Delta f/f) \times$ (Pk/Turb), for simple cones with various base angles. ● 20°, □ 30°, ○ 45°, △ 60°.

directions. This largest peak occurred within the first diameter downstream.

Fig. 4a shows $\Delta f/f$ vs Reynolds number for the simple cones. For the 20° cone, the frequency spread is more than 30%. Hence, the specification of the shedding period is not reliable to better than ±15%. The 60° cone with a frequency spread of 10% has the most consistent shedding frequency. The ratio $\Delta f/f$ decreases with increasing cone angle, but shows no systematic variation with Reynolds number.

The ratio Pk/Turb is plotted vs Reynolds number in Fig. 4b. It indicates the difficulties of laboratory observation through the requirement of large averaging times when this ratio is less than unity, as seen especially for the case of the 20° cone. No shedding was detected from a 10° cone.

The product of the two ratios,$(\Delta f/f)$ (Pk/Turb) is plotted vs Reynolds number in Fig. 4c. There is no clear-cut difference between the 45° and 60° cones, but there is a definite decrease toward lower values for the two cones with smaller angles.

Fig. 5 shows, for the composite cones, the three plots similar to those in Fig. 4. The very low values

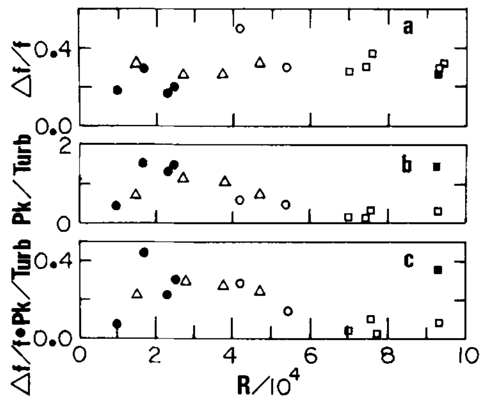

Fig. 5. Variation with Reynolds number of quantities related to vortex periodicity fluctuations, $\Delta f/f$, and to vortex shedding strength, $(\Delta f/f) \times$ (Pk/Turb), for complex cones. ○ 30° exponential, ● 45° exponential, □ 10°–20° double, ■ 20°–30° double, △ 45° twin.

of Pk/Turb for the 10°–20° cone indicates the great difficulty of experiments at small base angles.

The variation of the shed vortex strength with height is of interest in the laboratory experiments because the cloud patterns seen in the satellite pictures are associated with an inversion, which may, in principle, occur at any height. There being no simple way of finding the vortex axis or its strength (cf. Bloor and Gerrard, 1966), the height of the shedding peak as a function of the cross-stream direction was used as a guide. The distance between the points of maximum height on either side of the wake axis was used as a measure of the vortex location, and the maximum peak height was used as a measure of the vortex strength. For the 45° simple cone, at a downstream distance of about four base diameters, the maximum peak heights, on an arbitrary scale and at various distances z above the base plate, were as follows: at $z/h = 0.5$, 100; at $z/h = 0.75$, 100; at $z/h = 0.88$, 78; at $z/h = 1.0$, 36.

If the vortex axis is not perpendicular to the base plate, the separation of the two sides of the street will vary with height. In the atmospheric cases this would mean that this separation would depend on the cloud height and might vary from time to time unless the cloud height were always the same. Measurements with a 45° simple cone, taken downstream a little over one base diameter from the cone axis, gave an angle of 60° between the vortex axis and the base plate. At a downstream distance between three and four times the base diameter, the angle was 80°.

To study the decay of the wake vortices spectral measurements were made at a number of downstream locations for the 20°, 30° and 45° simple cones. If x_e is the distance in which the resonant peak is reduced by a factor $1/e$ and a is the downstream spacing of successive vortices, then x_e/a provides a useful number for comparison with the atmospheric results. For the 20°, 30° and 45° simple cones, respectively, x_e/a was 0.5, 1.2 and 1.9. The spacing a was estimated with the assumption that the wake speed was $0.8u_0$.

6. Discussion of the experiments

An important feature of the present experiments is the occurrence of only one shedding frequency. This is in contrast to Gaster's (1971) results for slightly tapered cylinders, from which shedding occurred in "cells" whose frequencies were related to the mean diameter of the cylinder over the length of the shedding cell. For cones with sufficiently steep sides, slopes greater than 60°, it is to be anticipated that more than one shedding frequency will be found.

The dimensional analysis summarized in Section 4 indicates for the simple cones a possible dependence of their Strouhal numbers on h/d. The cone base angle is related to h/d by $\tan\phi = 2h/d$; whence, from Fig. 2, it is seen that Strouhal number decreases as h/d increases. To provide an estimate of the base angle at which a second vortex frequency will develop, a straight line approximation at $R = 4 \times 10^4$ gives

$$S = 0.29 - 0.034 \tan\phi \qquad (9)$$

for $20° \leqslant \phi \leqslant 60°$. Extrapolation gives $\phi = 67°$ for $S = 0.21$, the value for an infinite cylinder. However, this limit cannot exist in actuality because of the prior appearance of a second shedding cell. Hence, it is likely that the second cell will first appear when the angle is near 70°.

Figs. 4c and 5c show that the strength of vortex shedding decreases as the slope angle decreases. Thus, although the shedding strength is about the same for 60° and 45° simple cones, it is somewhat lower for the 30° cone and considerably lower for the 20° cone. On the other hand, the likelihood that a 10° surface sheds very weakly as indicated in

Fig. 5c for the double cones. There the 10°–20° cone very clearly sheds with less strength than the 20°–30° cone. It is further noteworthy that the 10°–20° cone does not shed so strongly as the 20° simple cone. On the other hand, the 20°–30° cone has a somewhat greater shedding strength than the 30° simple cone. This suggests that the lower part of this double cone contributes significantly to the shedding of its 30° part, whereas the base plate, which may be thought of as having a 0° slope angle contributes very much less in the case of the 30° simple cone. The relative ineffectiveness of the smaller slope angles is also seen in Figs. 5c and 4c where the 20°–30° double cone has a greater shedding strength than the 20° simple cone, thus demonstrating the advantage of the steeper upper slope of this double cone. Fig. 5c shows that the shedding strengths of the exponential cones are nearly the same, a result apparently inconsistent with the observations for the other cone types. That the 30° exponential cone does not have a significantly lower shedding strength than the 45° exponential cone may be a consequence of differences in their profiles. The 30° cone is exponential only over the first one-third of its diameter and has a constant 15° slope thereafter. The 45° cone is exponential over its entire diameter and has slope angles less than 15° for the outer 54% of its diameter.

A comparison of the Strouhal numbers also shows the relative ineffectiveness of the lower parts of cones at small slope angles. If a cone is imagined to be made up of a pile of horizontal slices, each of which competes with the others to shed vortices at the shedding frequency of a cylinder of the same diameter, then the actual frequency will be determined by one of these slices, and the diameter of that slice will be d_{cyl}, the diameter of the equivalent cylinder. Therefore, if d_{co} is the characteristic diameter of the cone, the ratio d_{cyl}/d_{co}, given in Table 2, is a measure of the part of the cone most effective for shedding. Although this is a crude representation of the actual three-dimensional flow, it provides useful insights. The Strouhal number chosen for the equivalent cylinder was 0.212, the asymptotic value in the Roshko (1954) formula. For the simple cones, this ratio is greatest and the closest to 1.0 for the 60° cone. It is least for the 20° cone. This means that for simple cones with small angles the upper part of the cone is more effective in determining the shedding frequency than is the upper part of cones with large angles. For the two double cones, there is a dramatic difference, the cone with the lower slopes having a cylinder equivalent of only half the diameter of the cylinder equivalent of the 20°–30° cone. This result indicates that the upper section of 10°–20° cone is more effective in determining shedding frequency than the lower segment, even though the lower segment has a much larger area. The same can be said for the 20°–30° cone, but to a lesser extent. If this cone behaves like some kind of mean between 20° and 30° simple cones d_{cyl}/d_{co} should be between 0.73 and 0.8, whereas it is actually 0.6. The 30° exponential cone has a much smaller cylinder equivalent than the 45° expontial cone, a demonstration of the great effectiveness of the larger slope angles of the latter cone. Another way to view the exponential cone results is to note that $2b$ is the base diameter of a simple cone whose base angle is equal to θ_0. Table 2 shows that the 45° exponential cone is somewhat more effective than a simple cone of base diameter $2b$, whereas the 30° exponential cone is considerably less effective than the corresponding simple cone.

Table 2. *Observed mean Strouhal numbers of cones and cylinder-cone equivalents, d_{cyl}/d_{co}*

Type	Angle (deg.)	S_{mean}	d_{cyl}/d_{co}
Simple	20	0.29	0.73
	30	0.26	0.80
	45	0.26	0.80
	60	0.23	0.92
Double	10–20	0.70	0.30
	20–30	0.36	0.60
Exponential	30	0.29	0.73
	45	0.17	1.2
Twin	45	0.22	0.96

7. Cone models of volcanoes

Table 3 lists the mountain peaks modeled with the present laboratory results. They were chosen because their associated vortex shedding periods have been published (Tsuchiya, 1969; Lyons and Fujita, 1968; Thomson, Gower and Bowker, 1977) and because the required topographic information was available to the author. All but Cheju, an

Table 3. *Characteristics of volcano profiles and predicted periods of vortex shedding*

Volcano	Cone angle (deg.)	d_{sim} (km)	θ_0 (deg.)	$2b$ (km)	T_{sim} (h)	T_{exp} (h)	T_{twin} (h)	T_{meas} (h)
Cheju	5	31	10	23	2.9	2.1	—	4.4
Kiska	16	8.8	21	6.4	0.8	0.6	—	3.1
Pavlov	—	—	18	15	—	1.4	—	2.4
Pogromni	8	22	(a) 17 (b) 12	(a) 11 (b) 15	2.0	(a) 1.0 (b) 1.4	—	1.9
Shishaldin	22	14	24–35	10	1.3	0.9	3.0	2.8
Vsevidof	21	11	34–43	6.1	1.0	0.6	2.6	2.8

island south of the Korean peninsula, are in the Aleutian chain. Profiles or useable topographic information were published for Cheju (Tsuchiya, 1969), Kiska (Lyons and Fujita, 1968) and Pavlov (Thomson, Gower and Bowker, 1977). The profiles of the last three volcanoes in Table 3 were made directly from topographic maps of Unimak and Umnak islands. Wherever possible, the peaks were modeled by both a simple cone and an exponential cone. Where two or more peaks were close together, the twin-cone model was also used. The height of the simple cone model was the height of the peak above sea level, and the cone's base diameter was twice the volcano's diameter at an elevation equal to one-half of its peak height. The parameters for the exponential cone were found from a semi-log plot of the volcano profile, the ordinate being the logarithm of the height above sea level. A straight line was fitted to this plot.

In Table 3 the cone angle is the base angle for a simple cone; d_{sim} is the base diameter of a simple cone. The parameters for the exponential cone are θ_0 and $2b$. For Shishaldin, the highest of a row of three peaks on Unimak island, and for Vsevidof, the higher of a pair of peaks on Umnak island, two values of θ_0 are shown to indicate the asymmetries of their profiles. In these cones $2b$ is the sum of the "b" values for the two sides of the peaks. For Pogromni, a volcano for which an exponential is a rather poor fit, two sets of exponential parameters are listed. The choice (a) is from a mean line through a profile plot; whereas, the choice (b) places emphasis on the upper half of the peak. The profile of Pogromni is very close to that of a simple cone 1560 m high, truncated 160 m from the top. The small, isolated peaks on the plateau at the top of Pogromni are ignored. The only information available to the author for Mt Pavlov was published by Thomson, Gower and Bowker (1977) who give the peak height and its diameter at 750 m altitude. An exponential fit was made to this data to give the parameters listed in Table 3.

The volcano pair most nearly resembling the laboratory twin-cone model is Mt Vsevidof and Mt Recheshnoi. Simple cones were fitted to these two peaks, and the end-to-end distance at sea level was taken for the base diameter of their twin-cone equivalent. If the "percent overlap" is defined as the overlap distance at their bases of one simple cone by the other, divided by the base diameter of the first simple cone, then, the percent overlap of the laboratory twin-cone model is 50%. The percent overlap of Mt Vsevidof by Mt Recheshnoi is 56% and the overlap of Mt Recheshnoi by Mt Vsevidof is 39%. The twin-cone model for Shishaldin used simple cones fitted to Mt Shishaldin and Mt Isanotski. The percent overlap in this case is negative, −23%. The nearness of Mt Isanotski to Mt Roundtop, the smallest of the three peaks in the Shishaldin group, makes the twin-cone approximation arbitrary because there is no reason to believe that the three peaks might not shed vortices as a group, if Mt Shishaldin is not solely responsible for the observed vortices.

With the types of fitting discussed above, the base diameter of the simple cone is 1.39 times the exponential cone parameter $2b$, in the ideal case. The parameters in Table 3 give ratios close to 1.39 for all cases except those of Vsevidof and Pogromni, exponential case (a).

To choose the Strouhal number for modeling the volcanoes it is necessary to consider two difficulties. First, from Fig. 2 it is clear that S is still increasing at the highest value of R achieved in the laboratory; hence, a region of S independent of R has not been reached. Second, S increases as cone angle decreases, and the simple cone angles for the volcano models in Table 3 are equal to or less than the smallest angle, 20°, used in the laboratory. If the laboratory trends with R and S continue, then the appropriate S for modeling will be higher than the highest value, 0.3, found in the laboratory experiments. For the simple cone case it was decided to present in Table 3 the vortex shedding periods calculated with the use of a Strouhal number of 0.3, with the understanding that the periods are likely to be smaller than those shown. Hence, the disagreements between laboratory and atmospheric results may be greater, and the agreements are doubtful. Similar reasoning was applied to the exponential cone modeling, for which the Strouhal number selected was 0.3, the highest value for the 30° exponential cone. In the twin-cone case a Strouhal number of 0.22 was selected. References for the measured periods are given in Table 4.

Details of the atmospheric observations are listed in Table 4. In this table a is the distance between successively shed vortices and one side of the vortex street, u_e is the wake speed, u_0 is the environmental wind speed and d is the obstacle dimension used by the reporting authors to calculate the Strouhal number, S. T_{meas} is deduced from

$$T_{\mathrm{meas}} = (u_e/a) = (u_e/u_0)\,(u_0/a) \tag{3}$$

The measured quantities are u_0 and a, except for the Cheju case where both u_e and u_0 were measured. In the other cases authors have differed in their methods of finding u_e/u_0.

8. Conclusions

Table 3 shows that, with the exception of the simple cone case for Pogromni, the predicted periods for the simple cone and exponential models are significantly smaller than the measured periods. The twin-cone periods for the Shishaldin and Vsevidof groups are in good agreement with the measured periods. Hence, in three cases the volcanoes themselves provide adequate barriers to explain the observed vortex shedding period. That is, the vorticity created in the boundary layer near the surface of the volcanoes becomes rolled up into vortices in the wake on their lee sides. However, in three cases the volcanic peaks are much too small to account for the observations. In these cases, if the modeling criteria are satisfied, it can be concluded that stratification is not only important for the generation of these vortices, but the flow around the mountains is so altered by the stratification that either the Strouhal number for shedding from the mountain slopes is reduced, or the barrier enhancement effect discussed in Section 2 is such that vorticity generated in the atmosphere itself, well away from the mountains, is responsible for the vortex streets.

Other discrepancies, true for all the cases compared here, arise in the comparison of laboratory and atmospheric vortex streets. If the atmopheric wakes were as turbulent as those found in the laboratory, it is unlikely that the vortices would have been visible in the wake clouds. Furthermore, the non-dimensional decay distance, x_e/a, is very different in the two cases. As was seen in Section 5, $x_e/a = 0.5$ for the simple cone in the laboratory. But, $x_e/a \geqslant 6$, from calculations based

Table 4. *Characteristics of atmospheric wake vortices*

Feature	a (km)	u_e/u_0	d (km)	u_0 (m/s)	S	T_{meas} (h)
Cheju*	111	0.76	28	9.2	0.19	4.4
Kiska†	85	0.75	18	10.0	0.16	3.1§
Pavlov‡	65	0.75	18	10.0	0.21	2.4
Pogromni‡	50	0.75	13	10	0.20	1.9
Shishaldin‡	(c) 75	0.75	32	10	0.32	2.8
Vsevidof‡	(c) 75	0.75	17	10	0.17	2.8

* Tsuchiya, 1969; † Lyons and Fujita, 1968; ‡ Thomson et al., 1977.
§ Authors give 2.6.

on the atmospheric results presented by Thomson, Gower and Bowker (1977). These discrepancies in the decay distances lead to the conclusion that stratification of the atmosphere is important both for the formation and for the observation of the large number of vortices actually seen in cloud patterns.

The laboratory results make reasonable the search for vortex shedding from the volcanic peaks themselves and from similarly shaped mountain peaks even in the absence of stably stratified flow, although shorter periods are to be expected. Two considerations are important if such shedding is to be observed. First, large slope angles are more likely to produce significant shedding than small angles, as is apparent from the discussion in Section 6, of Figs. 4c and 5c and of the Strouhal number evidence. Second, the wake is likely to be turbulent, thereby masking and rapidly dissipating the vortex motion. Among the peaks listed in Table 3, Shishaldin and Vsevidof should be the best ones to study.

9. Acknowledgement

The author thanks S. Eskinazi of the Syracuse University Mechanical and Aerospace Engineering Department for helpful discussions.

REFERENCES

Batham, J. P. 1973. Pressure distributions on circular cylinders at critical Reynolds numbers. *J. Fluid Mech. 57*, 209–228.

Bloor, M. S. and Gerrard, J. H. 1966. Measurements on turbulent vortices in a cylinder wake. *Proc. Roy. Soc. 294*, 319–342.

Chopra, K. P. 1972. Velocity field in vortices leeward of islands. *J. Atmos. Sc. 29*, 396–399.

Chopra, K. P. and Hubert, L. F. 1964. Kármán vortex streets in earth's atmosphere. *Nature 203*, 1341–1343.

Chopra, K. P. and Hubert, L. F. 1965. Kármán vortex streets in wakes of islands. *AIAA Jour. 3*, 1941–1943.

Friday, E. W. Jr and Wilkins, E. M. 1967. Experimental investigations of atmospheric wake vortex trails. Essa Satellite Laboratory Research Grant E-41-67 (G). University of Oklahoma Research Institute, Dept. of Meteorology, Norman, Oklahoma.

Gaster, M. 1971. Vortex shedding from circular cylinders at low Reynolds numbers. *J. Fluid Mech. 46*, 749–756.

Greenly, G. D. Jr 1969. An investigation of the formation and maintenance of Kárman vortex patterns. M.Sc. Thesis, University of Oklahoma, Norman, Oklahoma. 48 pp.

Lyons, W. A. and Fujita, T. 1968. Mesoscale motions in oceanic stratus as revealed by satellite data. *Mon. Wea. Rev. 96*, 304–314.

Moussa, Z. M., Trischka, J. W. and Eskinazi, S. 1977. The near field in the mixing of a round jet with a cross-stream. *J. Fluid Mech. 80*, 49–80.

Mujumdar, A. S. and Douglas, W. J. M. 1970. Comment on "Vortex shedding from circular cylinders in sheared flow". *AIAA Jour. 8*, 990–991.

Roshko, A. 1954. On the drag and shedding frequency of two-dimensional bluff bodies. NACA Technical Note No. 3169, 1–29.

Snyder, W. H. 1972. Similarity criteria for the application of fluid models to the study of air pollution meteorology. *Boundary-Layer Meterol. 3*, 113–134.

Sykes, R. I. 1978. Stratification effects in boundary layer flow over hills. *Proc. Roy. Soc. Lond. A. 361*, 225–243.

Szecheny, E. 1975. Supercritical Reynolds number simulator for two-dimensional flow over circular cylinders. *J. Fluid Mech. 70*, 529–542.

Tennekes, H. and Lumley, J. L. 1972. *A first course in turbulence.* Cambridge, Mass.: The MIT Press, 98.

Thomson, R. E., Gower, J. F. R. and Bowker, N. W. 1977. Vortex streets in the wake of the Aleutian Islands. *Mon. Wea. Rev. 105*, 873–884.

Tsuchiya, K. 1969. The clouds with the shape of Kármán vortex streets in the wake of Cheju Island, Korea. *J. Meteor. Soc. Japan 47*, 457–464.

Zimmerman, L. I. 1969. Atmospheric wake phenomena near the Canary Islands. *J. Appl. Meteorology 8*, 896–907.

КОНИЧЕСКИЕ МОДЕЛИ ГОРНЫХ ПИКОВ, СВЯЗАННЫЕ С ВИХРЕВЫМИ ДОРОЖКАМИ В АТМОСФЕРЕ

Образование вихревых дорожек в атмосфере за горными пиками было промоделировано в однородном нестратифицированном потоке в аэродинамической трубе в следах за круглыми конусами различной формы и за одной комбинацией пары таких конусов. Предсказывается, что вихревые дорожки должны появляться в следах за изолированными пиками и за парой

близко расположенных пиков. Условия для образования вихрей тем предпочтительней, чем более круты склоны пиков. На основе лабораторных измерений и в предположении независимости от числа Рейнольдса предсказаны периодичности образования вихрей за шестью вулканическими пиками, для которых периодичности излучения вихрей были определены другими исследователями по спутниковым фотографиям облаков в подветренном потоке. Предсказанные периоды согласуются с измеренными в трех случаях и значительно меньше в трех других. Для последних сулчаев сделан вывод, что стратификация так меняет атмосферный поток, что или число Струхаля уменьшается или барьерный эффект топографического препятствия существенно усиливается. Делается также вывод, что стратификация, достаточная для уменьшения турбулентности, необходима для существования протяженной вихревой дорожки в атмосфере.